Uncertainty analysis of the optimal health-conscious operation of a hybrid PEMFC coastal ferry

*C. Dall'Armi, D. Pivetta, R. Taccani**

University of Trieste, Department of Engineering and Architecture, Via Valerio 10, Trieste, Italy

HIGHLIGHTS

- Health-conscious energy management strategy of hybrid PEMFC/LIB coastal ferry.
- Monte Carlo uncertainty analysis of the long-term operation of a hybrid ship.
- Global sensitivity analysis indicates hydrogen fuel cost as the most influent parameter.
- PEMFC/LIB degradation causes a 30% increase of hydrogen consumption at end of life.
- Variability of powertrain optimal power allocation decreases toward the end of life.

ARTICLE INFO

Article history:
Accepted 31 October 2021

Keywords:
Marine hydrogen fuel cells
PEMFC and LIB degradation
MILP optimization
Uncertainty analysis
Monte Carlo analysis

ABSTRACT

Hydrogen fueled Polymer Electrolyte Membrane Fuel Cells/Lithium-Ion Battery powertrains could be a promising solution for zero-local-emission shipping. The power allocation between PEMFC and LIB and their respective performance degradation play a crucial role in reducing the powertrain operating and maintenance costs. While several research works proposed energy management strategies to face these issues, a long-term operation optimization including the uncertainty in the input parameters of the model has not been extensively addressed. To this purpose, this study couples an operation optimization model of a PEMFC/LIB ferry propulsion system with a Monte-Carlo analysis to investigate the influence of PEMFC, LIB and hydrogen costs on the optimal operation of a hydrogen-powered ferry in the long-term. Hydrogen cost results to be the most influent parameter, in particular toward the end of the plant lifetime, when hydrogen consumption increases by up to 30%. Nevertheless, the variability of optimal ferry operation gradually decreases with the progressive PEMFC/LIB degradation.

Introduction

Non-governmental organizations, regulators, and ship-building companies are posing growing efforts to find strategies to reduce the emissions of the shipping sector, responsible today for about the 3% of total greenhouse gases emissions. Moreover, different long-term economic and energy scenarios foresee an increase of emissions by up to 30% in 2050 with respect to the 2008 levels [1]. There is evidence that alternative fuels and propulsion systems could help achieving the decarbonization of the shipping sector [2,3]. In particular, Polymer Electrolyte Membrane Fuel Cells (PEMFC) for ship propulsion are gaining attention as they can achieve zero-local-emission propulsion [4–8]. PEMFC-based propulsion systems usually encompass an Energy Storage

* *Corresponding author.*
E-mail address: taccani@units.it (R. Taccani).

System (ESS). Among different ESSs, Lithium-Ion Batteries (LIB) are often preferred given their high energy density. In particular, lithium iron phosphate (also called Lithium FerroPhosphate or LFP) chemistry is a mature technology for the shipping sector and has good performances in terms of safety onboard [9,10].

A drawback of such hybrid powertrains is their high cost, which affects not only the design but also the operation of the powertrain. Both PEMFC and LIB are subject to performance degradation that leads energy units to be less energy efficient over their lifetime and to be replaced more frequently than conventional powertrains (e.g., diesel internal combustion engines) [11]. By defining the optimal Energy Management System (EMS) it could be possible to increase PEMFC and LIB lifetimes, therefore reducing the replacement costs and hence improving the cost effectiveness of the whole plant. Several studies in the literature address the definition of the optimal EMS for hybrid PEMFC powertrains [12–18]. Most of these studies do not account for PEMFC and LIB degradation effects in the optimization model or take performance degradation into account only as a constraint in the optimization model, while only few studies set the minimization of power sources performance degradation as objective function of the optimization model [14,15]. Moreover, analyses on the progressive degradation of PEMFC and LIB over the entire lifetime have been rarely carried out [16]. Nevertheless, the mentioned studies adopt deterministic optimization approaches, where the uncertainty in the values of the input parameters is not considered. While this assumption is often adopted to limit the overall complexity of the optimization models, it does not give information on whether and how outputs of the optimization model are affected by the uncertainty characterizing the input parameters. On the contrary, uncertainty-based approaches, also known as stochastic approaches, allow to assess the effects of the input parameter uncertainties on the results of the optimizations.

Systematical uncertainty analyses have been identified as an emerging research topic in the modelling of energy systems [19]. This modelling approach is particularly suitable for modelling renewable energy systems, where the intrinsic stochasticity of renewable energy sources (e.g. sun and wind) poses serious challenges in the correct predictability of the robustness of results. In addition, renewable energy technologies are often characterized by high level of uncertainties in the capital costs, given their innovative nature [20,21]. In this context, some authors proposed uncertainty analyses of stationary energy systems accounting for the intrinsic uncertainty related on the costs of the new technologies [22–27]. For example, Lee et al. [22] performed an economic evaluation of an electrolysis plant for hydrogen production under uncertainty. They used a Monte Carlo (MC) methodology to estimate the impact of the system uncertainty on the final cost of produced hydrogen. They particularly focused on uncertainty in the prices of hydrogen production equipment, electricity, labor, and construction. Mavromatidis et al. [23] characterized the uncertainty of 27 parameters involved in the model of a distributed energy system, among which the energy carrier prices, the emission factors and the investment costs. Petkov et al. [24] performed an uncertainty analysis on the design optimization of a power-to-hydrogen multi-energy system, considering uncertainty linked not only to the energy demand but also to the investment costs and the lifetime of the energy units. Radaideh et al. [25] performed a design optimization under uncertainty of two hybrid fuel cell energy system for power generation and cooling purposes. They applied different methods to perform the uncertainty and sensitivity analyses, among which MC sampling for the uncertainty propagation and regression-based sensitivity analysis. Radaideh et al. [26] proposed the sensitivity analysis and uncertainty quantification on a solid oxide fuel cell system to understand how uncertain design parameters in input affect the power output and system efficiency.

With regard to ship power systems energy modelling, uncertainty analyses have been mainly performed to evaluate the power system performances under different operating conditions, with the aim of assessing the robustness of models. Uncertainty of the sailing profile is often considered, as it affects the overall energy balance of the ship [28,29]. For instance, Coraddu et al. [29] performed a MC analysis to estimate the energy efficiency of a ship propulsion system as a function of displacement and speed. Other aspects, as the weather conditions, cost of equipment, and hull fouling could be also included as uncertainty input parameters in the optimization of the energy system. Tillig et al. [30] reported that the highest uncertainties in predicting optimal speeds and fuel savings are caused by uncertainties in the prediction of weather condition and economic factors. Hull fouling of the ship's hull introduces speed losses and hence contributes to increase the uncertainty in the simulation model results [31].

Although the analysis of the impact of uncertain power plant components costs could be interesting especially for energy systems encompassing new technologies, it appears to be a lack of studies in the literature that address uncertainty analyses on power plant components costs and fuel costs for ship energy systems. Concerning hybrid PEMFC/LIB ship propulsion systems, the analysis of how uncertainty in the costs affects the energy model could be fundamental not only in the design phase, but also to determine the best EMS. In fact, the results of uncertainty analysis for the long-term operation of a hybrid PEMFC/LIB powertrain could lead to a comprehensive view of operating and maintenance costs variability over its lifetime. In addition, given the low industrial maturity of PEMFC and LIB for marine use and the not-widespread use of hydrogen as fuel for mobility, the variability in technologies and fuel costs could significantly influence the power allocation and hence the optimal operation of the powertrain during the ship operation. In order to address these aspects and hence fill this literature gap, the present study proposes an uncertainty analysis of the optimal health-conscious operation of a hydrogen-fueled hybrid PEMFC/LIB ship propulsion system. Uncertainties on power plant components and hydrogen costs have been considered in the analysis. A small size ferry for coastal navigation has been taken as case study since this type of vessels could particularly benefit from the installation of hydrogen-fueled propulsion systems [3], even if the proposed methodology has a general validity. The uncertainty analysis has been carried out by coupling a two-layers Mixed-Integer Linear Programming (MILP) health-conscious optimization model with a MC sampling analysis. A Global Sensitivity Analysis (GSA) has then been performed to determine which parameter influences the most the output of the optimization.

Methodology

This section presents a thorough description of the proposed methodology. A simplified schematic of the methodology is shown in Fig. 1. Firstly, uncertainty characterization has been performed for the input parameters of the model, namely the cost of hydrogen fuel (c_{H2}), cost of LIB (c_{batt}) and cost of PEMFC (c_{FC}). Afterwards, multi-objective optimizations have been performed to find the optimal daily operation of the hybrid ferry taken as a case study with reference to the operating cost. The operating cost includes the fuel and degradation of the power plant. The optimal sizes of the energy conversion and storage units for the ferry have been determined by using the optimization tool developed in a previous study [14]. The main characteristics of the ferry as well as its daily power demand profile have been reported in Appendix B.

A two-layer approach has been used for the optimization (*Phase 2*): an internal layer (*Ageing dependent layer*) for the health-conscious operation optimization of one day representative of a specific month, and an external layer (*Time dependent layer*) to evaluate the progressive degradation of PEMFC and LIB over the plant lifetime. Once either PEMFC or LIB have reached the End of Life (EoL), the optimization is stopped. For each month, optimization results have provided information about (i) plant lifetime estimation, (ii) operating cost, and (iii) power flows in the representative days. Lastly, a sensitivity analysis has been conducted on the optimization outputs to identify the most influent input parameters.

Uncertainty characterization of input parameters

Uncertainty Characterization (UC) has been carried out to identify the uncertain parameters and to determine the probability associated with each value of the uncertain parameters [23]. For the specific case of maritime PEMFC/LIB powertrains fueled by hydrogen, three main uncertainties have been proposed, related to: cost of hydrogen fuel (c_{H2}), cost of LIB (c_{batt}) and cost of PEMFC (c_{FC}).

The uncertainty on the proposed input parameters has been evaluated by analyzing data available in the literature.

Once the range of values that can be assumed by the input parameters has been determined, the data have been analyzed through a PERT distribution to assess the probability linked to each value. Among different probability functions, PERT distribution has been chosen since it is often used to model expert's opinion [32], as for example data from technical report, datasheet or research papers, and has already been used in similar analyses, as for example in Ref. [24]. Differently from uniform or triangular distributions, the shape of the PERT distribution is more similar to a normal distribution, with a smoother shape around the mode.

PERT distribution has been defined for the three uncertain parameters by using the algorithm *pertdist* implemented in Python [33]. Such algorithm requires in input the lowest and highest values assumed by the uncertain parameters, and the mode. Table 1 reports such values for the selected parameters, namely the hydrogen cost c_{H2}, the PEMFC stack cost c_{FC}, and the LIB cost c_{batt}. The relative probability distributions of the

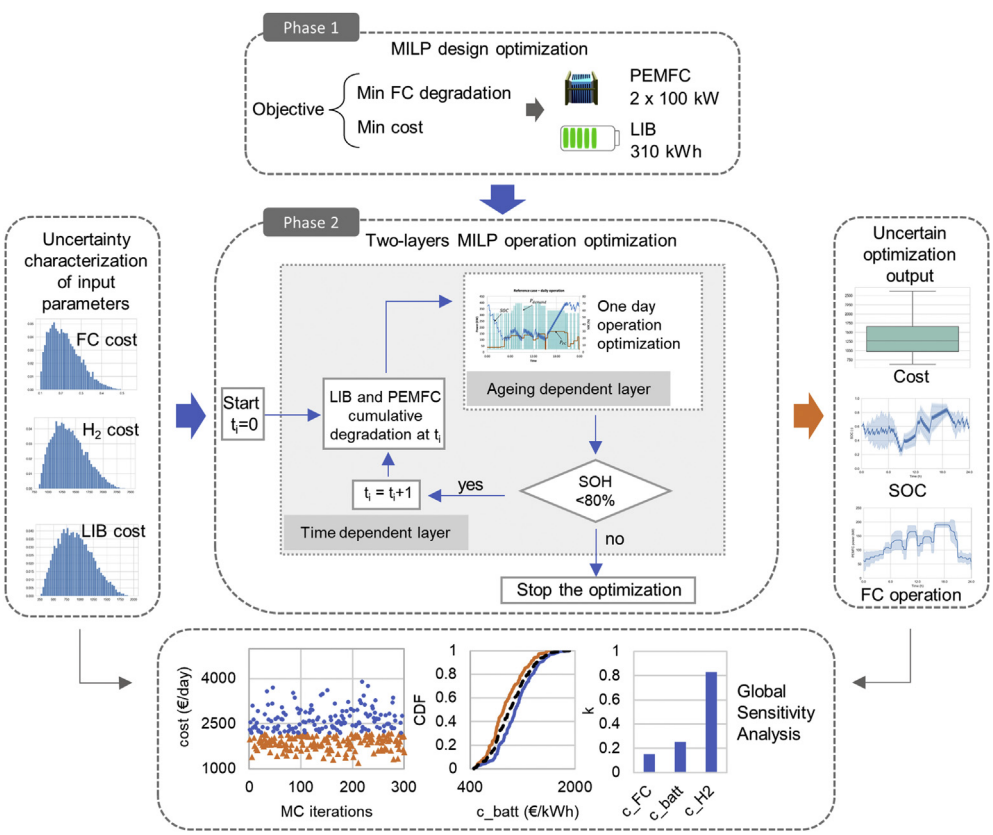

Fig. 1 – Simplified schematic of the proposed methodology.

parameters are shown in Fig. 2. Both Table 1 and Fig. 2 show a high variability of the parameters, once again demonstrating the importance of the analysis proposed in the paper.

Monte Carlo analysis

The influence of uncertain input parameters on the optimization results has been evaluated by performing a Monte Carlo (MC) analysis over the energy system lifetime. At each MC iteration, random values of the uncertain parameters are sampled from their respective probability distribution (see Fig. 2) and enter the optimization model. By increasing the number of the MC iterations, it is possible to cover as many combinations of uncertain parameters as possible, without the *a priori* definition of different scenarios. Once all the MC iterations have been completed, the results of the MILP optimization can be extrapolated with the relative degree of uncertainty, i.e. it can be evaluated the confidence through which it is possible to define the optimal operation of the plant. Considering the overall complexity of the optimization model, the number of MC iterations (n_{MC}) has been set equal to 300 for each month of the plant lifetime. The number of MC iterations has been chosen to find a good compromise between the time required to solve the optimization problem and the convergence of results. This last aspect is dealt within the Appendix A.

Optimization model

Before starting to optimize the ferry operation for the entire plant lifetime (Fig. 1, *Phase 2*), a design optimization has been conducted to determine the best sizes of both LIB and PEMFC (Fig. 1, *Phase 1*) that minimize the investment cost, the daily operating cost, and the PEMFC degradation. In this section the main equations of the optimization model have been reported for a better understanding of the hybrid system operation and of the uncertainty analysis results proposed in this study. For a comprehensive description of the methodology adopted to find the optimal design of the energy system the author is referred to Ref. [14]. Note that in the *Phase 1* a deterministic optimization approach has been followed, and the mean values of the uncertain input cost parameters (Table 1) have been considered.

The PEMFC rated power and the LFP battery energy capacity enter as fixed input parameters in the second phase optimization for the definition of the best EMS. As proposed in Ref. [16], the operation optimization has been set to concurrently minimize three objective functions: fuel consumption (f_1 in Eq. (1)), PEMFC performance degradation (f_2 in Eq. (2)), and LFP battery performance degradation (f_3 in Eq. (3)). The optimization problem has been written in Python [46] and solved with the MILP optimizer Gurobi Optimization [47]. For the multi-objective optimization, Gurobi solver requires in input the weight of each objective functions. In this way, the objective functions have been combined linearly in a single-objective function (f_{MO} in Eq. (4)), which can be seen as the total daily operating cost of the ferry.

$$f_1 = \sum_{j=1}^{n} \int_0^{t_{fin}} F_{FC_j}(t)dt \tag{1}$$

$$f_2 = \sum_{j=1}^{n} \int_0^{t_{fin}} dV_j(t)dt \tag{2}$$

$$f_3 = \int_0^{t_{fin}} Q_{loss\ battery}(t)dt \tag{3}$$

$$f_{MO} = Minimize(w_1 \cdot f_1 + w_2 \cdot f_2 + w_3 \cdot f_3) \tag{4}$$

where, for the j-th PEMFC stack, $\int_0^{t_{fin}} F_{FC_j}(t)dt$ is the consumption of hydrogen in the time interval between 0 and t_{fin}, and $\int_0^{t_{fin}} dV_j(t)dt$ is the total voltage degradation. $\int_0^{t_{fin}} Q_{loss\ battery}(t)dt$ is the loss of energy capacity for the LFP battery. w_1, w_2 and w_3 are the weights for the three objective functions.

The weights have been expressed in terms of costs related to each objective function, as shown in Eqs. (5)–(7).

$$w_1 = c_{H_2} \tag{5}$$

$$w_2 = c_{FC} \cdot \frac{P_{FC_{max}}}{V_{loss_{max}}} \tag{6}$$

$$w_3 = c_{batt} \cdot \frac{E_{battery,max}}{Q_{loss_{max}}} \tag{7}$$

where $P_{FC_{max}}$ is the PEMFC rated power, $V_{loss_{max}}$ is the total voltage loss permitted for the single cell of the PEMFC stacks (set equal to 20% of the reference maximum voltage for a new PEMFC, namely $V_{ref,FC}$), $E_{battery,max}$ is the energy capacity of the LFP battery, $Q_{loss_{max}}$ is the maximum capacity fade of the battery (set equal to 20% of the energy capacity).

Firstly, the power balance for the proposed hybrid powertrain is shown in Eq. (8). It has been assumed that the powertrain fulfills the power required by the ferry over a typical daily operation for each time *t*. The power demand has a 3-min resolution.

$$\sum_{j=1}^{n} P_{FC_j}(t) + P^{+}_{batt}(t) = P_{demand}(t) + P^{-}_{batt}(t) \tag{8}$$

Table 1 – Characterization of uncertain parameters entering as input in the optimization model.

Parameter	Unit	min	max	mode	mean	Ref.
c_{H2}	€/kWh	0.12	0.55	0.20	0.25	[34–37]
c_{FC}	€/kW	830	2500	1000	1222	[4,13,38–41]
c_{batt}	€/kWh	400	2000	950	933	[9,13,42–45]

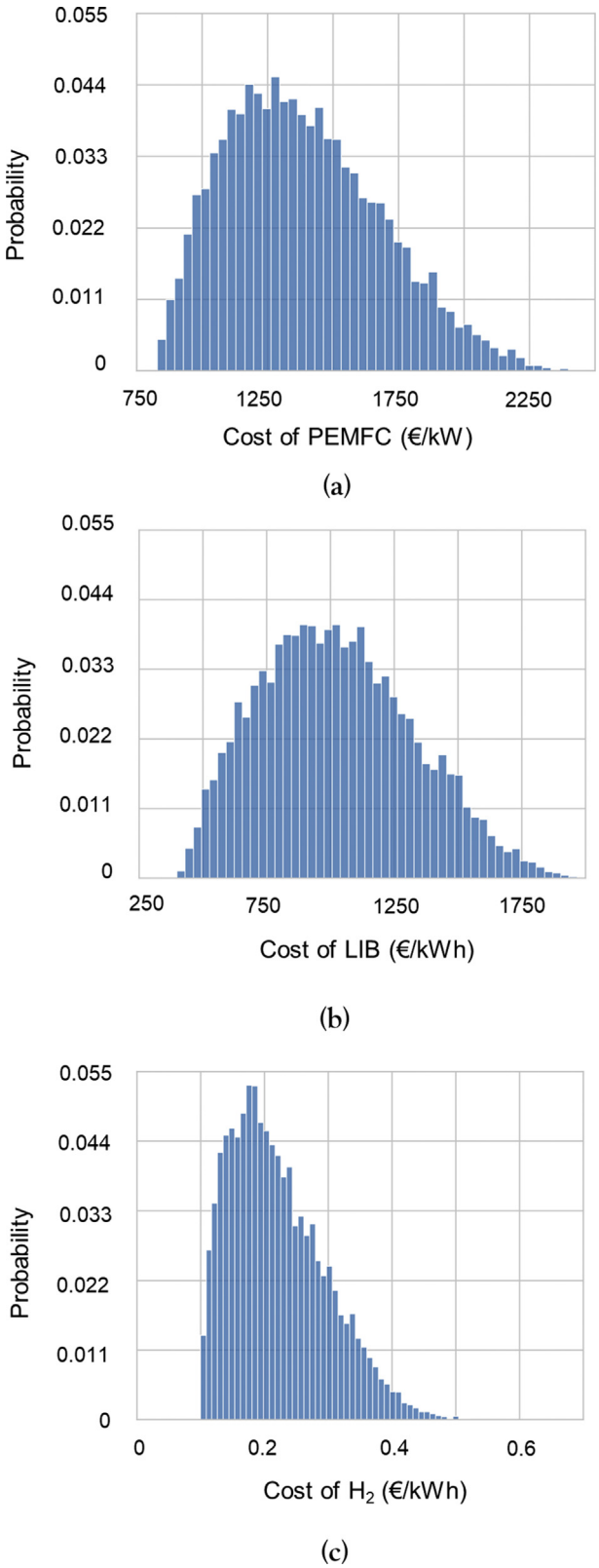

Fig. 2 – PERT distributions of uncertain parameters: (a) PEMFC cost (c_{FC}), (b) LIB cost (c_{batt}), and (c) H_2 cost (c_{H2}).

where $P_{FC_j}(t)$ is the power provided for the j-th PEMFC stack, $P^{+}_{batt}(t)$ is the power provided by the battery, $P_{demand}(t)$ is the power required by the ferry, $P^{-}_{batt}(t)$ is the charging power of the battery.

The main equations describing the operation of the PEMFC are shown in Eqs. (9)–(11).

$$F_{FC_j}(t) = \left(k_{1_F} \cdot I_{FC_j}(t) + k_{2_F}\right) \cdot \delta_{FC_j}(t) + \delta_{st,up_j}(t) \cdot F_{start} \cdot P_{FC_{max}} \tag{9}$$

$$P_{FC_j} = \left(k_{1_P} \cdot I_{FC_j}(t) + k_{2_P}\right) \cdot \delta_{FC_j}(t) \tag{10}$$

$$\eta_{FC} = P_{FC_j} \Big/ F_{FC_j} \tag{11}$$

where I_{FC_j} is the current density for the j-th PEMFC stack, k_{1F}, k_{2F}, k_{1P} and k_{2P} are the linearization coefficients used to describe the characteristic operation curves with linear equations. For the j-th PEMFC stack, δ_{FC_j} is the binary variable defining on/off status or the inclusion/exclusion, δ_{st,up_j} is the binary variable defining the occurrence of a start-up phase, F_{start} is the fuel required in a start-up phase, η_{FC} is the energy efficiency (based on the lower heating value of hydrogen).

As for LIB, the Eq. (12) reports the equation describing the energy stored in LIB at each time-step t, while Eq. (13) expresses the State Of Charge (SOC) of LIB at each time step.

$$E_{batt}(t) = E_{batt}(t-1) + \left(\eta_{batt} \cdot P^{-}_{batt}(t) - (1/\eta_{batt}) \cdot P^{+}_{batt}(t)\right) \cdot \Delta t \tag{12}$$

$$SOC(t) = \frac{E_{batt}(t)}{E_{battery_{max}}} \tag{13}$$

where $E_{batt}(t)$ and $E_{batt}(t-1)$ are the energy stored in the battery at time t and $(t-1)$, η_{batt} is the charging/discharging efficiency, Δt is the considered time resolution for the problem (3 min).

Lastly, the State Of Health (SOH) has been calculated for the j-th PEMFC stack (SOH_{FC_j}) and for the LIB (SOH_{LIB}) as shown in Eqs. (14) and (15), respectively.

$$SOH_{FC} = \frac{V_{ref,FC} - \int_0^{t_{fin}} dV_j(t)dt}{V_{ref,FC}} \tag{14}$$

$$SOH_{LIB} = \frac{E_{battery,max} - \int_0^{t_{fin}} Q_{loss\ battery}(t)dt}{E_{battery,max}} \tag{15}$$

Global sensitivity analysis

Once obtained the results of the MC iterations, a sensitivity analysis has been conducted to obtain an estimation of the parameters that mostly influence the optimization problem. Four methods are normally used to perform the sensitivity analysis: (i) local methods, (ii) regression-based methods, (iii) screening methods, and (iv) variance-based methods (or global methods) [21]. A Global Sensitivity Analysis (GSA) has been chosen in this study as it allows to consider the information linked to the stochasticity of input parameters. A MC Filtering (MCF) has been performed through the application of the two-sample Kolgmogorov-Smirnov (KS) test. Such an approach is often used for this type of problems as it allows to quantify how much a parameter influences the output of the problem [24,48]. The optimization results have been divided into two subsets: a *behavioral* subset B for the objective function results under the median, and a *non-behavioral* subset $\overline{B}$ for the objective function results above the median.

Once obtained the B and $\overline{B}$ subsets of the MC results, each sample of the n_{MC} input parameters has been split into two subsets according to the associated B or $\overline{B}$ result, and the relative Cumulative Distribution Functions (CDFs) have been built and compared. The goal of this phase is to demonstrate or confute the null hypothesis formulated as: "*Do the CDFs of the B and $\overline{B}$ subsets belong to the same distribution of the input parameter i?*". Whenever the null hypothesis is demonstrated, the CDFs of the B and $\overline{B}$ subsets will appear similar, and the parameter will be flagged as *non-influent* for the model: each value of $x^{(i)}$ could equally result in B or $\overline{B}$ model output. On the contrary, if the CDFs of the B and $\overline{B}$ subsets are different, i.e. the null hypothesis is confuted, the parameter $x^{(i)}$ will be flagged as *influent* for the model, as some values of $x^{(i)}$ are more likely to return B outputs and others $\overline{B}$. To quantify the *similarity* between the two CDFs, the KS test requires the calculation of the parameter k, defined as in Eq. (16):

$$k = \max\left|F\left(x^{(i)}|B\right) - F\left(x^{(i)}|\overline{B}\right)\right| \tag{16}$$

where $F(x^{(i)}|B)$ and $F(x^{(i)}|\overline{B})$ are the CDFs of the B and $\overline{B}$ subsets, respectively.

Afterwards, the parameter k has been compared with the critical parameter D, defined as in Eq. (17):

$$D = c(\alpha)\cdot\sqrt{\frac{n_B + n_{\overline{B}}}{n_B n_{\overline{B}}}} \tag{17}$$

where n_B and $n_{\overline{B}}$ are the number of elements in the B and $\overline{B}$ subsets of the parameter $x^{(i)}$, and the constant $c(\alpha)$ is defined according to the significance level α as reported in Ref. [49].

Table 2 reports the values of D at different significance levels α.

Whenever the parameter k is lower than or equal to D the parameter is defined as non-influent, while if k is higher than D the parameter is flagged as influent. In this study, the significance level α has been set to 0.01 to avoid incorrect estimations of the influent parameters, as suggested by Ref. [48]. Hence, the reference value of the critical parameter D to be considered in the GSA is 0.19.

Results and discussion

In this section, the main results of the operation optimization model are presented and discussed. The optimal design of the hybrid PEMFC/LIB powertrain has been evaluated by applying the methodology proposed in Ref. [14] with mean values of the uncertain input parameters c_{H2}, c_{FC}, and c_{batt} (reported in Table 1). The resulting optimal sizes of 200 kW for PEMFC and 310 kWh for LIB have been used for performing the operation optimization.

Table 2 – Values of the critical parameter D for different significance levels α. The values considered for the GSA in this study are reported in bold.

α	0.1	0.05	0.02	**0.01**
D	0.14	0.16	0.17	**0.19**

Plant lifetime and daily operating cost

At first, the estimation of the plant lifetime has been retrieved from the optimization model outputs with reference to the mean values of SOH_{FC} and SOH_{LIB}, i.e. the mean values of the results obtained from the n_{MC} MC iterations of the optimization model.

Fig. 3 shows the mean SOH of PEMFC and LIB, and the mean cost over the entire lifetime of the plant. It can be noticed that the proposed power plant can operate for 23 consecutive months, i.e. 690 days. After this time, both PEMFC (black dots in Fig. 3) and LIB (white dots in Fig. 3) reach a SOH of 80% and hence the EoL. Contextually, from Fig. 3 it can be inferred that the mean operating cost of the ferry (i.e. f_{MO} in Eq. (4), indicated with squares in Fig. 3) tends to increase, reaching a daily mean cost at the 23rd month that is about 16% higher than the daily operating cost at the first month. Moreover, it should be noticed that the increase of the mean cost has a non-linear trend (solid line in Fig. 3). This is mainly due to the progressive decrease of PEMFC efficiency and hence to the increase of hydrogen consumption over the plant lifetime. As shown in Fig. 4, which reports the daily ferry hydrogen consumption over time, the hydrogen consumption at the 23rd month is

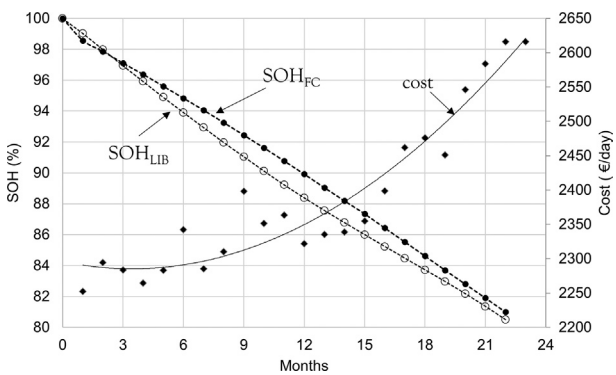

Fig. 3 – Mean daily operating cost (◆) of the ferry over the entire plant lifetime (f_{MO} in Eq. (4)), mean SOH of LIB (○) and mean SOH of PEMFC (●) over the plant lifetime. Mean values have been calculated on the basis of the results of n_{MC} optimizations.

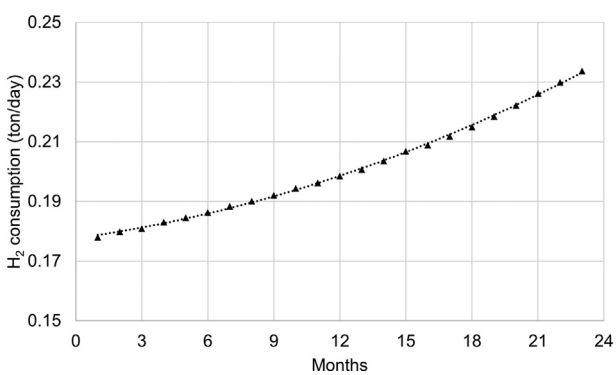

Fig. 4 – Mean daily hydrogen consumption (▲). Mean values have been calculated on the basis of the results of the n_{MC} optimizations.

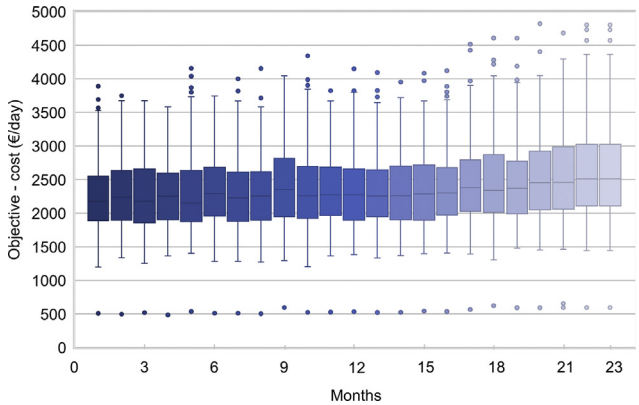

Fig. 5 – Results of the operating cost of the ferry over the entire plant lifespan. Boxplots extend from the first quartile (25%) to the third quartile (75%) of the cost results obtained by the n_{MC} model optimizations for each month. Solid lines in the boxes represent the mean cost at each month. Solid lines outside the boxes extend from the lower to the upper limit of the samples, and dots indicate the outliers.

about 30% higher than the fuel consumption at the first month. Such aspects will be further discussed in Section Global sensitivity analysis of optimization results.

As for costs, it is also interesting to see how the uncertainty on the input parameters affects the optimization model outputs. Fig. 5 reports the boxplots of the objective function f_{MO} (Eq. (4)) as retrieved from the n_{MC} iterations. The boxes contain the central 50% of cost distribution resulting for the n_{MC} optimizations at each month. In other words, boxes extend from the first (25%) to the third quartile (75%) of each sample. The mean values are represented by the solid lines in the boxes. The dots indicate the outliers, and the lines outside the boxes extend from the lower to the upper limit of the samples. In addition to the tendency of costs to increase over the plant lifetime already discussed, Fig. 5 points out how the objective function results are affected by the variability of the input parameters. It can be observed that variability on the optimization results increases with the progressive ageing of the plant. At the beginning of the plant lifetime, the central 50% of cost results are spread in a ~500 € range, while at the end this amplitude increases by up to ~1000 € range.

Optimal operation of batteries and fuel cells over the entire lifetime

As previously described for operating costs, the proposed methodology also allows to have an outlook on the variability of the optimal operation (i.e. the optimal EMS) of the hybrid powertrain over the plant lifetime. Fig. 6 reports the SOC of LIB over one typical day of operation, representative of one

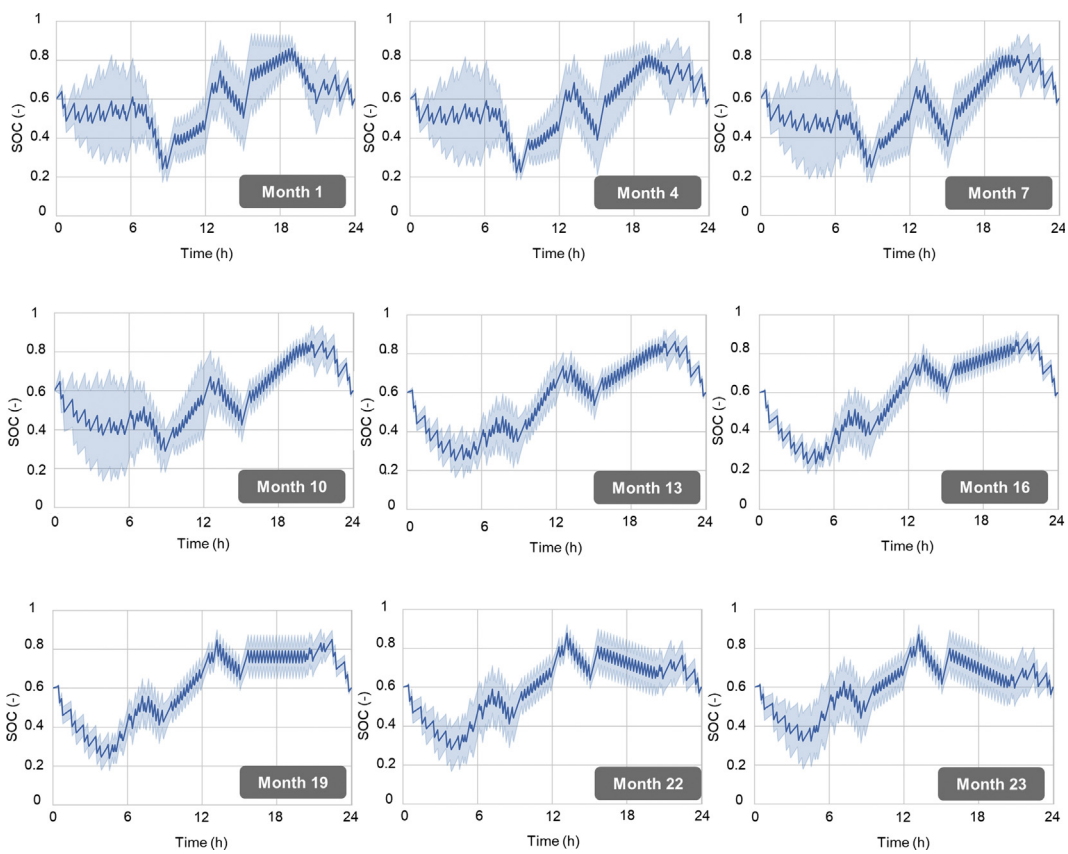

Fig. 6 – Optimal SOC of LIB over a typical day of operation, representative of each month. Solid lines represent the mean value of SOC at each time-step. Shaded blue areas indicate the uncertainty linked to the calculated value, expressed in terms of standard deviation, as resulting from the n_{MC} values of the variables at each time-step. (For interpretation of the references to color in this figure legend, the reader is referred to the Web version of this article.)

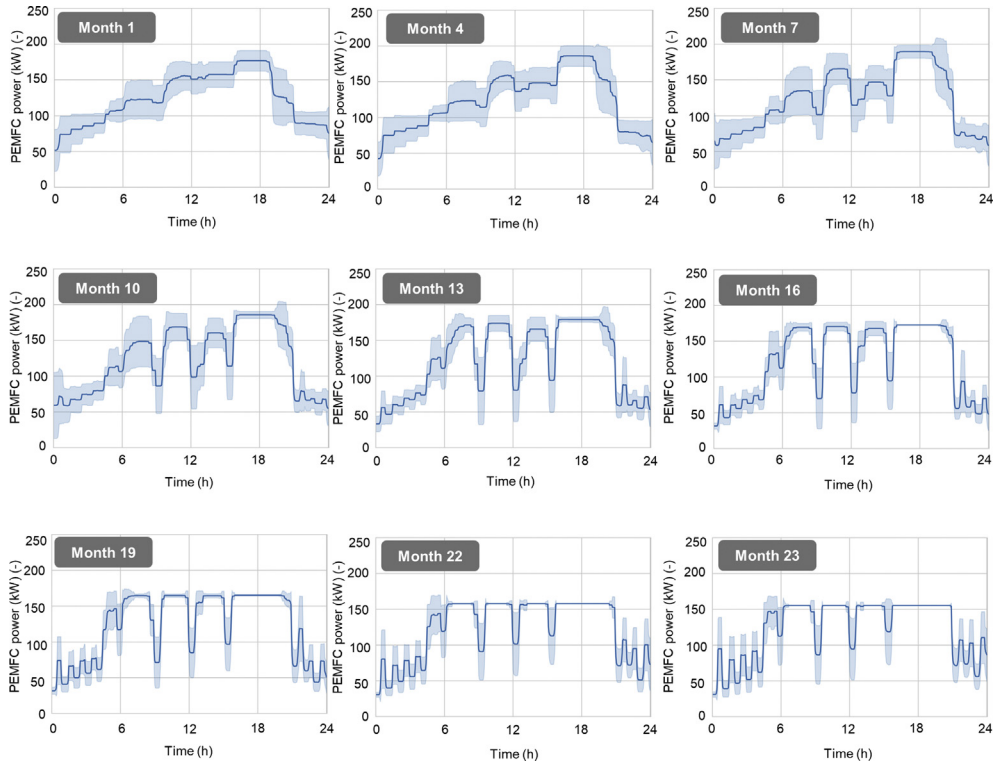

Fig. 7 – Optimal PEMFC power over a typical operation day, representative of each month. Solid lines represent the mean value of P_{FC} at each time-step. Shaded blue areas indicate the uncertainty linked to the calculated value, expressed in terms of standard deviation, as resulting from the n_{MC} values of the variables at each time-step. (For interpretation of the references to color in this figure legend, the reader is referred to the Web version of this article.)

month. Similarly, Fig. 7 shows the PEMFC power in a typical day. In both Figs. 6 and 7, the solid lines represent the mean values of either *SOC* or P_{FC} at each time-step (Eqs. (10) and (13)) in Section Optimization model), while the light blue areas indicate the uncertainty linked to the calculated values, expressed in terms of standard deviation, as resulting from the n_{MC} values of the variables at each time-step. For the sake of simplicity in the figures, results have been reported only for nine over 23 months of operation. Looking at the mean values in Fig. 7, it can be noted that PEMFC generally tend to avoid the operation at rated power and frequent start-up phases, as these would result in higher degradation rates (i.e. worsening the objective function f_2 in Eq. (2)). The ideal health-conscious operation of PEMFC would be at constant load, but the EMS operates to find a compromise that allows to limit the LIB degradation as well. At the beginning of the plant lifetime, the EMS will advantage the PEMFC, as they are the components with the highest cost (see Table 1). However, with the progressive degradation of LIB over time, the influence of $c_{batt} \cdot f_3$ on the objective function f_{MO} increases. As a consequence, with the passing of time the EMS will allow a higher degradation rate of PEMFC to limit the LIB degradation. For both LIB and PEMFC, it can be noticed that the variability in the optimal operation is higher at the beginning of the plant lifetime. This trend is opposite to the one of the operating cost in Fig. 5. For example, at the first month different input parameters can lead to even substantially different optimal operations of the plant, but this does not reflect in a high variability of the overall operating cost in Fig. 5. In fact, at the beginning of the plant lifetime, the PEMFC are not degraded and hence can operate at high efficiency. As a consequence, even large variations in the cost of hydrogen would not cause large variations in the resulting cost. Also, at the first month both PEMFC and LIB are new, and hence the degradation rate is lower than the one at EoL: different operational pathways would hence not result in largely different cost outputs in terms of costs

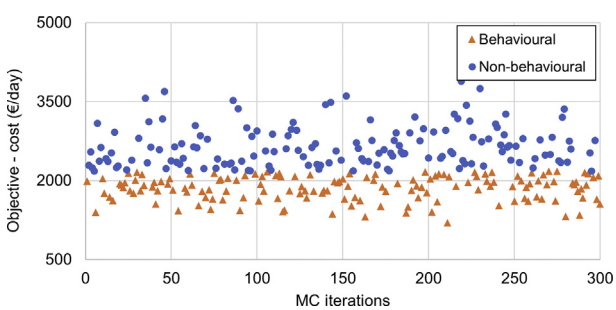

Fig. 8 – Results of the MC filtering for the first month of vessel operation. Orange triangles indicate the behavioral subset of the n_{MC} cost results (cost below the median). Blue dots represent the cost results of the non-behavioral subset (cost above the median). (For interpretation of the references to color in this figure legend, the reader is referred to the Web version of this article.)

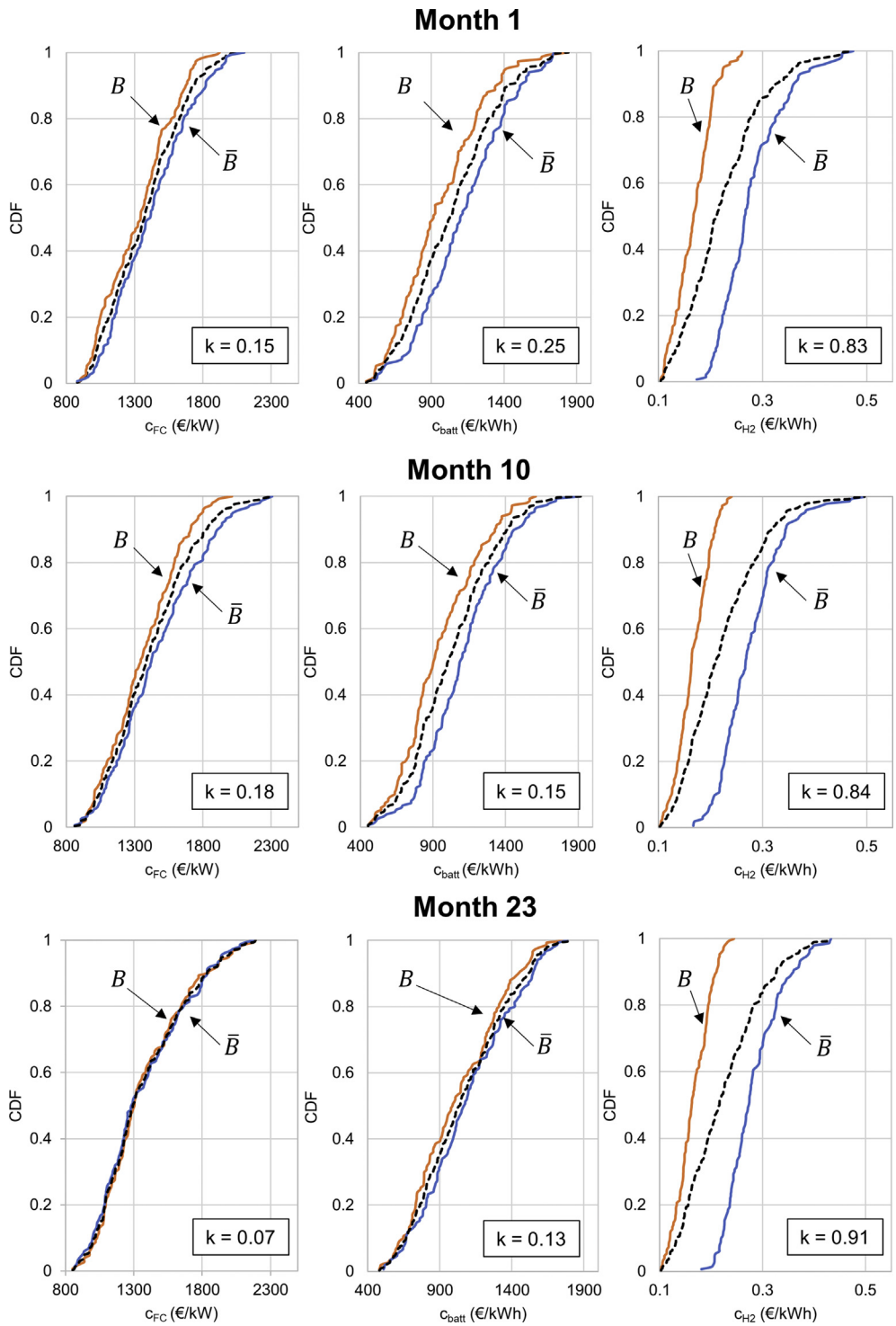

Fig. 9 – GSA results for 1st, 10th and 23rd months of operation. The orange lines represent the CDF of the input parameter values which led to cost result in the *B* (behavioral) subset. The blue lines indicate the cumulative distribution functions of the input parameter values which lead to cost result in the $\bar{B}$ (non-behavioural) subset. The dashed black lines represent the cumulative distribution functions of the entire sample of the input parameters. (For interpretation of the references to color in this figure legend, the reader is referred to the Web version of this article.)

associated to the degradation rates. On the contrary, looking at the 23rd month (i.e. the last month of operation), the optimal EMS does not have a large variability despite the variability of input parameters. Nevertheless, the aged PEMFC have lower efficiency, and hence even a small variation in the hydrogen cost in input can result in a large variation of the

operating cost. To better justify what said till now, the next section presents the GSA.

Global sensitivity analysis of optimization results

The GSA has been conducted for every month of the ferry operation to identify the input parameter that influences the most the optimization results. For each month, the n_{MC} results of the operating cost have been divided into two subsets: a behavioral subset B for costs under the median and a non-behavioral subset $\overline{B}$ for costs above the median. The results of this first step of the GSA have been reported for the first month in Fig. 8 as an example, but similar results have been obtained for each month.

Once obtained the B and $\overline{B}$ subsets of the objective function, the corresponding samples of uncertain input parameters have been divided accordingly, and CDF have been derived for each parameter. Fig. 9 shows the CDF of the behavioral and non-behavioral subsets of the uncertain parameters c_{FC}, c_{batt} and c_{H2} for the first, 10th and 23rd months. The orange lines indicate the CDF of the input parameter values which lead to cost result in the B subset, while the blue lines indicate the CDF of the input parameter values which lead to cost result in the $\overline{B}$ subset. For each parameter, values of the k indicator (Eq. (16)) are reported in the boxes. It can be noticed that for all the months the most influent parameter is the cost of hydrogen c_{H2}, while c_{FC} and c_{batt} have k values that are similar to the critical value D (0.19). Moreover, the analysis throughout the whole plant lifetime points out that the influence of c_{H2} on the objective function increases with the passing of time (higher values of k). This is due to the progressive performance degradation of the plant, in particular the PEMFC degradation, that causes a decrease in the mean efficiency and hence an increase in the consumption of hydrogen per day. Such considerations also explain the increase of costs over time, as seen in Fig. 4 in Section Plant lifetime and daily operating cost.

Conclusions

The proposed study has investigated the effects of uncertain input parameters on the long-term operation optimization of a hybrid PEMFC/LIB ship propulsion system. The analysis addressed some of the issues emerged from the literature review on this subject, being able to optimize the energy management system of the powertrain taking into account the progressive ageing of the components over the entire plant lifetime, evaluating the effects of uncertain input parameters on the results of the developed optimization model. While the optimization of energy management system operation is dealt with in some research works, an uncertainty analysis of PEMFC, LIB and hydrogen costs is not extensively addressed in this field. Hence, the originality of this paper lies in the development of an optimization methodology able to quantitatively evaluate the influence of different parameters in the health-conscious energy management of an innovative hybrid PEMFC/LIB ship power system. The main contributions of the present study can be summarized as follows:

- the global sensitivity analysis quantitatively demonstrated that the cost of hydrogen is the most influent parameter on the comprehensive cost objective function;
- the mean daily operating cost increases by up to 16% with the progressive degradation of the plant; this is due to the progressive decrease of the plant efficiency and the hence the increase hydrogen consumption; consequently, the cost of hydrogen increases its influence on the objective function over powertrain lifetime;
- the daily hydrogen consumption increases over time due to the progressive degradation of PEMFC and LIB; at the last month (23rd) the daily hydrogen consumption is about 30% higher than the consumption at the first month;
- at the beginning of the plant lifetime, the uncertainty on input parameters can lead to a high variability of the optimal PEMFC and LIB operation, but this does not reflect in high uncertainty in the daily operating cost (spread in a ~500 € range) given the limited degradation rates of PEMFC and LIB when they are new;
- at the end of the plant lifetime the optimal operation of PEMFC and LIB does not have a large variability despite the variability of input parameters. However, given the degraded performance of PEMFC, even a small variation in the hydrogen cost in input can result in a large variation of the operating cost (spread in a ~1000 € range).

Overall, it can be concluded that the proposed study was able to give risk-aware information on the optimal plant operation over the entire lifetime for uncertain input parameters.

A further development of this study could address the uncertainty analysis on the power demand of the ferry, i.e. on the mission profile. Moreover, a tool to optimize the design of hybrid fuel cell powertrains under uncertainty could be developed, considering the entire lifetime of the plant, and could be used for other types of vessels.

Declaration of competing interest

The authors declare that they have no known competing financial interests or personal relationships that could have appeared to influence the work reported in this paper.

Appendix A

Figure A1 shows the mean daily operating cost resulting from the uncertainty analysis performed with different numbers of MC iterations. It can be inferred that the choice of performing the uncertainty analysis with $n_{MC} = 300$ represents a good trade-off between the quality of the obtained results and the overall computational effort.

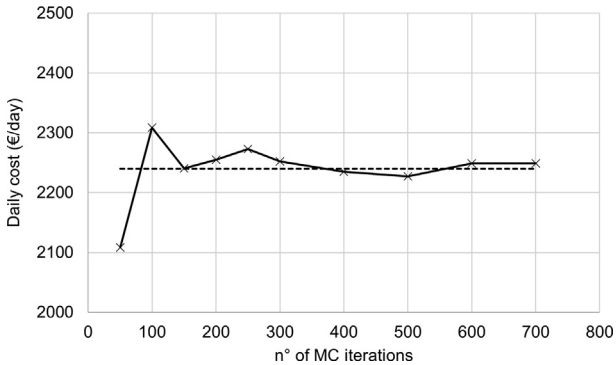

Figure A1 Mean daily operating cost obtained by performing the uncertainty analysis with increasing numbers of MC iterations. The solid line represents the daily mean cost at varying numbers of MC iterations. The dashed line indicates the average value of daily cost among the different numbers of MC iterations.

Appendix B

Table B1 reports the main characteristics of the small size ferry for coastal navigation taken as case study for the proposed analysis, while Figure B1 shows the power demand profile of the ferry during a typical day of operation. Power system volume and weight in Table B1 have been elaborated basing on available data on diesel ICE powertrain for marine propulsion, scaled to fit into the ferry installed power. The average voyage duration and the number of voyages performed by the ferry in a day have been assumed basing on typical operational schedules. For more information on the ferry the reader is referred to a previous publication [14], which also reports an exhaustive description of the proposed PEMFC/LIB architecture.

Table B1 – Main characteristics of the small size ferry for coastal navigation chosen as case study [14].

	Unit	Value
Length overall	m	42
Breadth extreme	m	9
Gross tonnage	t	280
Installed power – propulsion	kW	2 × 206
Installed power – auxiliary engines	kW	2 × 28
Power system volume	m^3	15.5
Power system weight	kg	7185
Average voyage duration	min	5
n° of voyages per day	–	72

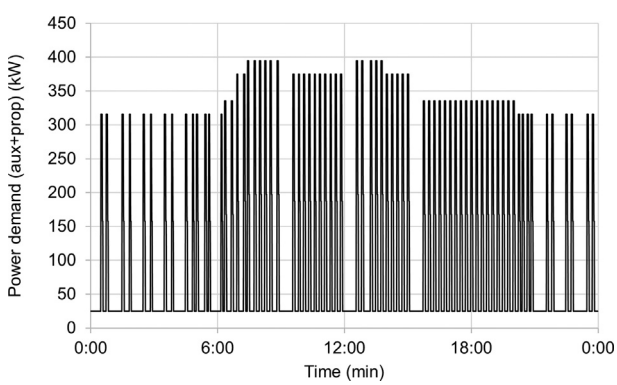

Figure B1 Power demand profile of the ferry during a typical day of operation [14].

REFERENCES

[1] nternational Maritime Organization (IMO). Fourth greenhouse gas study 2020. n.d, https://www.imo.org/en/OurWork/Environment/Pages/Fourth-IMO-Greenhouse-Gas-Study-2020.aspx. [Accessed 22 June 2021].

[2] Bicer Y, Dincer I. Clean fuel options with hydrogen for sea transportation: a life cycle approach. Int J Hydrogen Energy 2018;43:1179–93. https://doi.org/10.1016/j.ijhydene.2017.10.157.

[3] Nazir H, Muthuswamy N, Louis C, Jose S, Prakash J, Buan MEM, et al. Is the H2 economy realizable in the foreseeable future? Part III: H2 usage technologies, applications, and challenges and opportunities. Int J Hydrogen Energy 2020;45:28217–39. https://doi.org/10.1016/j.ijhydene.2020.07.256.

[4] van Biert L, Godjevac M, Visser K, Aravind PV. A review of fuel cell systems for maritime applications. J Power Sources 2016;327:345–64. https://doi.org/10.1016/j.jpowsour.2016.07.007.

[5] Dall'Armi C, Micheli D, Taccani R. Comparison of different plant layouts and fuel storage solutions for fuel cells utilization on a small ferry. Int J Hydrogen Energy 2021;46:13878–97. https://doi.org/10.1016/j.ijhydene.2021.02.138.

[6] De-Troya JJ, Álvarez C, Fernández-Garrido C, Carral L. Analysing the possibilities of using fuel cells in ships. Int J Hydrogen Energy 2016;41:2853–66. https://doi.org/10.1016/j.ijhydene.2015.11.145.

[7] McKinlay CJ, Turnock SR, Hudson DA. Route to zero emission shipping: hydrogen, ammonia or methanol? Int J Hydrogen Energy 2021;46:28282–97. https://doi.org/10.1016/j.ijhydene.2021.06.066.

[8] Gadducci E, Lamberti T, Bellotti D, Magistri L, Massardo AF. BoP incidence on a 240 kW PEMFC system in a ship-like environment, employing a dedicated fuel cell stack model. Int J Hydrogen Energy 2021;46:24305–17. https://doi.org/10.1016/j.ijhydene.2021.04.192.

[9] EMSA. Study on electrical energy storage for ships. EMSA - European Maritime Safety Agency; 2020.
[10] COBRA compact battery rack - becker marine systems. n.d, https://www.becker-marine-systems.com/products/product-detail/becker-cobra-compact-battery-rack.html. [Accessed 13 July 2021].
[11] Vichard L, Steiner NY, Zerhouni N, Hissel D. Hybrid fuel cell system degradation modeling methods: a comprehensive review. J Power Sources 2021;506:230071. https://doi.org/10.1016/j.jpowsour.2021.230071.
[12] Chen H, Zhang Z, Guan C, Gao H. Optimization of sizing and frequency control in battery/supercapacitor hybrid energy storage system for fuel cell ship. Energy 2020;197:117285. https://doi.org/10.1016/J.ENERGY.2020.117285.
[13] Wu P, Bucknall R. Hybrid fuel cell and battery propulsion system modelling and multi-objective optimisation for a coastal ferry. Int J Hydrogen Energy 2020;45:3193–208. https://doi.org/10.1016/j.ijhydene.2019.11.152.
[14] Pivetta D, Dall'Armi C, Taccani R. Multi-objective optimization of hybrid PEMFC/Li-ion battery propulsion systems for small and medium size ferries. Int J Hydrogen Energy 2021. https://doi.org/10.1016/j.ijhydene.2021.02.124.
[15] Zhang Z, Guan C, Liu Z. Real-time optimization energy management strategy for fuel cell hybrid ships considering power sources degradation. IEEE Access 2020;8:87046–59. https://doi.org/10.1109/ACCESS.2020.2991519.
[16] Dall'Armi C, Pivetta D, Taccani R. Health-conscious optimization of long-term operation for hybrid PEMFC ship propulsion systems. Energies 2021;14:3813. https://doi.org/10.3390/EN14133813.
[17] Yue M, Jemei S, Gouriveau R, Zerhouni N. Review on health-conscious energy management strategies for fuel cell hybrid electric vehicles: degradation models and strategies. Int J Hydrogen Energy 2019;44:6844–61. https://doi.org/10.1016/J.IJHYDENE.2019.01.190.
[18] Balestra L, Schjølberg I. Energy management strategies for a zero-emission hybrid domestic ferry. Int J Hydrogen Energy 2021. https://doi.org/10.1016/j.ijhydene.2021.09.091.
[19] Frangopoulos CA. Recent developments and trends in optimization of energy systems. Energy 2018;164:1011–20. https://doi.org/10.1016/j.energy.2018.08.218.
[20] Yue X, Pye S, DeCarolis J, Li FGN, Rogan F, Gallachóir B. A review of approaches to uncertainty assessment in energy system optimization models. Energy Strategy Rev 2018;21:204–17. https://doi.org/10.1016/j.esr.2018.06.003.
[21] Radaideh MI, Radaideh MI. Application of stochastic and deterministic techniques for uncertainty quantification and sensitivity analysis of energy systems. 2019.
[22] Lee B, Heo J, Choi NH, Moon C, Moon S, Lim H. Economic evaluation with uncertainty analysis using a Monte-Carlo simulation method for hydrogen production from high pressure PEM water electrolysis in Korea. Int J Hydrogen Energy 2017;42:24612–9. https://doi.org/10.1016/j.ijhydene.2017.08.033.
[23] Mavromatidis G, Orehounig K, Carmeliet J. Uncertainty and global sensitivity analysis for the optimal design of distributed energy systems. Appl Energy 2018;214:219–38. https://doi.org/10.1016/j.apenergy.2018.01.062.
[24] Petkov I, Gabrielli P. Power-to-hydrogen as seasonal energy storage: an uncertainty analysis for optimal design of low-carbon multi-energy systems. Appl Energy 2020;274:115197. https://doi.org/10.1016/j.apenergy.2020.115197.
[25] Radaideh MI, Radaideh MI, Kozlowski T. Design optimization under uncertainty of hybrid fuel cell energy systems for power generation and cooling purposes. Int J Hydrogen Energy 2020;45:2224–43. https://doi.org/10.1016/j.ijhydene.2019.11.046.
[26] Radaideh MI, Radaideh MI. Efficient analysis of parametric sensitivity and uncertainty of fuel cell models with application to SOFC. Int J Energy Res 2020;44:2517–34. https://doi.org/10.1002/er.4837.
[27] Lane B, Reed J, Shaffer B, Samuelsen S. Forecasting renewable hydrogen production technology shares under cost uncertainty. Int J Hydrogen Energy 2021;46:27293–306. https://doi.org/10.1016/j.ijhydene.2021.06.012.
[28] Vrijdag A. Estimation of uncertainty in ship performance predictions. J Mar Eng Technol 2014;13:45–55. https://doi.org/10.1080/20464177.2014.11658121.
[29] Coraddu A, Figari M, Savio S. Numerical investigation on ship energy efficiency by Monte Carlo simulation. Proc Inst Mech Eng Part M J Eng Marit Environ 2014;228:220–34. https://doi.org/10.1177/1475090214524184.
[30] Tillig F, Ringsberg JW, Psaraftis HN, Zis T. Reduced environmental impact of marine transport through speed reduction and wind assisted propulsion. Transport Res Transport Environ 2020;83:102380. https://doi.org/10.1016/j.trd.2020.102380.
[31] Coraddu A, Oneto L, Baldi F, Cipollini F, Atlar M, Savio S. Data-driven ship digital twin for estimating the speed loss caused by the marine fouling. Ocean Eng 2019;186:106063. https://doi.org/10.1016/j.oceaneng.2019.05.045.
[32] Vose D. Risk analysis: a quantitative guide. John Wiley & Sons; 2008.
[33] Python documentation for PERT distribution pertdist. n.d, https://pypi.org/project/pertdist/. [Accessed 8 July 2021].
[34] DNV G. Assessment of selected alternative fuels and technologies. 2019.
[35] Ishimoto Y, Voldsund M, Nekså P, Roussanaly S, Berstad D, Gardarsdottir SO. Large-scale production and transport of hydrogen from Norway to Europe and Japan: value chain analysis and comparison of liquid hydrogen and ammonia as energy carriers. Int J Hydrogen Energy 2020;45:32865–83. https://doi.org/10.1016/j.ijhydene.2020.09.017.
[36] Acar C, Dincer I. Comparative assessment of hydrogen production methods from renewable and non-renewable sources. Int J Hydrogen Energy 2014;39:1–12. https://doi.org/10.1016/j.ijhydene.2013.10.060.
[37] Madsen RT, Klebanoff LE, Caughlan SAM, Pratt JW, Leach TS, Appelgate TB, et al. Feasibility of the zero-V: a zero-emissions hydrogen fuel-cell coastal research vessel. Int J Hydrogen Energy 2020;45:25328–43. https://doi.org/10.1016/j.ijhydene.2020.06.019.
[38] IEA. International Energy Agency. The future of hydrogen. Data and assumptions; 2019.
[39] Zeng Y, Cai Y, Huang G, Dai J. A review on optimization modeling of energy systems planning and GHG emission mitigation under uncertainty. Energies 2011;4:1624–56. https://doi.org/10.3390/en4101624.
[40] Staffell I, Green R. The cost of domestic fuel cell micro-CHP systems. Int J Hydrogen Energy 2013;38:1088–102. https://doi.org/10.1016/j.ijhydene.2012.10.090.
[41] Raucci C. The potential of hydrogen to fuel international shipping. Dr Thesis. UCL (University Coll London); 2017.
[42] Tsiropoulos I, Tarvydas D, Lebedeva N. Li-ion batteries for mobility and stationary storage applications - scenarios for costs and market growth. EUR 29440 EN. Luxemb: Publ Off Eur Union; 2018. https://doi.org/10.2760/87175. JRC113360, . [Accessed 3 June 2021].
[43] Nykvist B, Nilsson M. Rapidly falling costs of battery packs for electric vehicles. Nat Clim Change 2015;5:329–32. https://doi.org/10.1038/nclimate2564.
[44] Wu P, Bucknall R. Marine propulsion using battery power. In: Shipp Chang Clim Conf 2016; 2016.

[45] Zhou Z, Benbouzid M, Charpentier JF, Scuiller F, Tang T, Zhou Z, et al. A review of energy storage technologies for marine current energy systems. Renew Sustain Energy Rev 2013;18:390–400. https://doi.org/10.1016/j.rser.2012.10.006ï.
[46] Python website. n.d. https://www.python.org/. [Accessed 13 July 2021].
[47] Gurobi website. n.d. https://www.gurobi.com/. [Accessed 13 July 2021].
[48] Mavromatidis G. Model-based design of distributed urban energy systems under uncertainty. PhD Thesis. 2017.
[49] O'Connor PD, Kleyner A. Practical reliability engineering. 2011.